



**Michigan  
Technological  
University**

Michigan Technological University  
**Digital Commons @ Michigan Tech**

---

Dissertations, Master's Theses and Master's Reports

---

2021

## Nonlinear Model Predictive Control of Wave Energy Converter

Isha Malekar

*Michigan Technological University, imalekar@mtu.edu*

Copyright 2021 Isha Malekar

---

### Recommended Citation

Malekar, Isha, "Nonlinear Model Predictive Control of Wave Energy Converter", Open Access Master's Report, Michigan Technological University, 2021.  
<https://doi.org/10.37099/mtu.dc.etr/1222>

Follow this and additional works at: <https://digitalcommons.mtu.edu/etr>



Part of the [Controls and Control Theory Commons](#), and the [Ocean Engineering Commons](#)

NONLINEAR MODEL PREDICTIVE CONTROL OF WAVE ENERGY  
CONVERTER

By

Isha S. Malekar

A REPORT

Submitted in partial fulfillment of the requirements for the degree of

MASTER OF SCIENCE

In Mechanical Engineering

MICHIGAN TECHNOLOGICAL UNIVERSITY

2021

© 2021 Isha S. Malekar

This report has been approved in partial fulfillment of the requirements for the Degree of MASTER OF SCIENCE in Mechanical Engineering.

Department of Mechanical Engineering-Engineering Mechanics

Report Advisor: *Dr. Gordon G. Parker*  
Committee Member: *Dr. Wayne W. Weaver*  
Committee Member: *Dr. Chee-Wooi Ten*  
  
Department Chair: *Dr. William W. Predebon*

## Table of Contents

List of Figures .....	iv
List of Tables .....	v
List of Abbreviations .....	vi
Abstract .....	viii
1 Introduction.....	1
1.1 Assumptions .....	2
2 Wave Energy Converter Model .....	4
2.1 Point Absorber Introduction.....	4
2.2 Static and Dynamic Nonlinear Froude-Krylov Forces.....	6
3 Model Predictive Controller .....	8
4 Results And Discussions.....	10
4.1 Bang-Bang Control in MPC .....	10
4.2 MPC In Regular Waves.....	13
4.3 Comparison of Nonlinear and Linear MPC Results.....	14
5 Conclusion .....	15
6 References.....	16

## List of Figures

Figure 2.1. Spherical buoy point absorber WEC.....	4
Figure 2.2. Sign conventions for forces acting on spherical buoy of WEC.....	5
Figure 3.1. Block diagram of MPC for WEC.....	8
Figure 4.1.1. Bang-bang control of WEC with PTO force limit of $\pm 5000$ N.....	10
Figure 4.1.2. PTO force and velocity with PTO limits $\pm 150000$ N.....	11
Figure 4.1.3. Comparison of displacement for PTO force limits of $\pm 150000$ N Vs $\pm 5000$ N.....	11
Figure 4.1.4. Comparison of velocity for PTO force limits of $\pm 150000$ N Vs $\pm 5000$ N.....	12
Figure 4.1.5. Comparison of energy absorbed with PTO force limits $\pm 5000$ N and $\pm 150000$ N.....	12
Figure 4.2.1. Comparison of displacement of WEC buoy for linear MPC vs NLMPC – regular waves.....	13
Figure 4.2.2. Energy absorbed in linear MPC and NLMPC for regular waves.....	14

## List of Tables

Table 2.1 WEC parameters used to simulate spherical buoy.....	7
Table 3.1 MPC parameters used in simulation.....	9
Table 3.2 Constraints used for MPC simulation.....	9

## List of Abbreviations

$m$  – Mass of buoy

$\mu$  – Added mass

$z$  – Displacement of buoy

$\rho$  – Water density

$R$  – Radius of buoy

$h_o$  – Draft of buoy

$\eta$  – Free surface elevation

$\dot{z}$  – Velocity

$\ddot{z}$  – Acceleration

$B$  – Radiation damping coefficient

$K_h$  – Hydrostatic stiffness coefficient

$F_{exc}$  – Wave excitation force

$F_h$  – Hydrostatic stiffness force

$F_R$  – Radiation force

$F_{pto}$  – Power take off force/ generator force

$MPC$  – Model Predictive Controller

$J$  – MPC cost function

$NLMPC$  – Nonlinear Model Predictive Controller

$LMPC$  – Linear Model Predictive Controller

$FK\ force$  – Froude-Krylov Force

$fkS_{nl}$  – Froude-Krylov hydrostatic nonlinear force

$fkS_{lin}$  – Froude-Krylov hydrostatic linear force

$fkD_{nl}$  – Froude-Krylov hydrodynamic nonlinear force

$f_{kS_{lin}}$  – Froude-Krylov hydrodynamic linear force



## Abstract

In this report model predictive control (MPC) is applied to a simulated, spherical, point absorber wave energy converter to maximize energy extraction. Constraints are applied to the buoy's displacement and the power take-off (PTO) generator force. The WEC's "truth" model uses nonlinear Froude-Krylov (FK) hydrostatic and hydrodynamic forces. This is in contrast with previous studies where linear approximations are used in the form of a hydrostatic stiffness force and a wave excitation force. The nonlinear forces become significant when the vertical displacement of the buoy exceeds about 40% of the buoy's radius. Two versions of MPC are compared where optimal PTO forces are calculated based on (1) a linear model, called LMPC, and (2) the nonlinear model, called NLMPC. For the cases considered, the energy absorbed using NLMPC is greater than for LMPC. Furthermore, the linear MPC solution, when applied to the truth model.

# 1 Introduction

Coal, natural gas, petroleum, and diesel fuels, used in electricity production, release carbon dioxide, carbon monoxide, sulfur dioxide with detrimental effects on the environment. According to US Energy Information Administration (EIA), renewable energy will be the most used energy by the year 2050 [1]. Wave energy converters can harvest energy 90% of the time [2]. Water wave energy is one of the renewable energy sources which is periodic and predictable and travels large distances with little to no energy loss [3]. To harvest wave energy, research ongoing to develop different types of Wave Energy Converters (WECs) such as oscillating water columns, overtopping devices, point absorbers, and surging devices to name a few [3].

A WEC's power take-off (PTO) converts wave kinetic energy into electrical energy. It has been shown that to maximize energy extraction a WEC's PTO should be controlled, where at times it is used as an actuator instead of its primary role as a generator [4]. Candidate control strategies, such as latching and impedance matching, have difficulties in providing state-constrained solutions where the buoy is expected to move greater than is physically possible. Here, state constrained optimization is used to implement these constraints using Model Predictive Control (MPC) where the cost function is the net energy extracted over the control horizon.

## Model Predictive Control –

One of the earliest papers on MPC was by Gilbert et al. where they postulated using an optimization process to affect closed-loop control. At each control update time, an optimal control problem is solved  $T$  seconds into the future. The first, zero-order held, optimal actuator command is then sent to the system as the input. The process continues as long as the control system is in operation. While some dynamic systems have closed-form optimal control solutions, most do not. Since numerical optimal control solutions can be computationally slow, implementation of MPC has only become feasible in recent years with the advent of high-performance embedded processors and fast optimization solvers. An attractive feature of MPC is that the optimal control solution can be subject to the physical constraints of the system. However, this makes finding an optimal solution in real-time a potential problem. Feasibility may be all that can be achieved at times.

Control systems often seek to reject external disturbances. In contrast, a WEC controller must exploit the wave forces, which can be viewed as a disturbance, to extract energy. Thus, knowing the wave forces, over the control horizon, helps with the implementation of a WEC MPC solution. Forecasting wave excitation forces has been accomplished using several methods including a Kalman filter [6], autoregressive (AR) models [7-8], and neural networks [9]. Since the focus of this study is on the differences between linear MPC (LMPC) and nonlinear MPC (NLMPC), the wave force prediction problem is removed by considering perfect knowledge of wave elevation, not wave forces, over the control horizon. The goal of MPC is to maximize energy flow into WEC. Based on known future excitation force, motion, and PTO force constraints, the objective function of the optimization problem is set to maximize the absorption of incident wave energy.

Researchers have used a linear model of wave radiation force i.e. system that uses a simple linear damper [6]. But the research has been done on implementing radiation convolution terms used in the state-space form [5][10][11]. This report will use a simple linear model of wave radiation with “B” radiation damping coefficient like the one used by Brekken for both LMPC and NLMPC [6].

NLMPC uses actual nonlinear Froude-Krylov forces subjected to WEC buoy. The nonlinear FK forces are nonlinear hydrostatic and hydrodynamic forces. In LMPC, the nonlinear hydrostatic and hydrodynamic forces are linearized and solved around the equilibrium position of the buoy. One of the reasons to use such a linearized model is to avoid simulating computationally expensive problem.

But as the problem is solved around the equilibrium position of the buoy, at the higher amplitudes of motion, error in actual hydrostatic and hydrodynamic forces buoy is subjected and linearized FK forces used by LMPC increases. This error is not captured by the LMPC and gives incorrect control force to WEC. LMPC, controlling the nonlinear WEC plant gives less amount of energy absorbed. This is the potential problem with using LMPC to control WEC.

To avoid this problem, NLMPC uses nonlinear FK forces [11]. The NLMPC model uses the instantaneous wetted surface area to calculate the exact nonlinear hydrostatic stiffness force and nonlinear hydrodynamic force. NLMPC thus takes into account the nonlinear hydrostatic and hydrodynamic forces subjected to WEC buoy and calculates the correct PTO force to keep buoy motion within defined state constraints and maximize the energy extraction.

NLMPC proves to be a good choice for controlling WEC subjected to high amplitudes of motion.

## 1.1 Assumptions

A spherical, point absorber WEC is considered. The main assumptions exploited are –

1. The PTO is ideal where the energy flow into the WEC is given by

$$E = - \int_0^T F_{pto} \cdot \dot{z} \, dT$$

where  $F_{pto}$  is the PTO force and  $\dot{z}$  is the WEC's vertical speed. The positive sense of both quantities is upward.

2. The buoy's incident wave time history is known in the future consistent with the control horizon. To put this into perspective, the control horizon in the example below is set to 3 seconds or half wave period.
3. The radiation force of waves is a linear approximation and radiation damping is approximated from WAMIT data.

4. Added mass is the mass of fluid surrounding the buoy which is accelerated with buoy displacement is approximated to a value and calculated from WAMIT data.
5. Only displacement and PTO force are constrained in the MPC optimization problem. Future work will include adding a constraint on velocity.

## 2 Wave Energy Converter Model

After introducing the spherical, point absorber wave energy converter the model approach is summarized and the model assumptions are provided. This is followed by a more detailed description of the model terms.

### 2.1 Point Absorber Introduction

Consider the WEC below that uses a spherical buoy and a power take-off device (PTO) whose base is fixed to the seafloor. The waves cause the buoy to oscillate vertically resulting in relative velocity between the PTO's top and bottom. This provides an opportunity to convert kinetic energy into electrical energy. In this study, the PTO is considered ideal and can flow power both into and out of the buoy which is assumed to only move vertically. It's well known that adding energy to the buoy, in a carefully controlled manner, can result in greater net extraction over several periods of oscillation. The model predictive controller (MPC) described later will seek to apply a force to the buoy that maximizes the energy extraction or  $-\int_0^T F_{pto} \cdot \dot{z}(t) dt$

where  $T$  is the control horizon,  $F_{pto}$  is the force applied to the buoy by the PTO and  $\dot{z}(t)$  is the buoy's vertical speed.

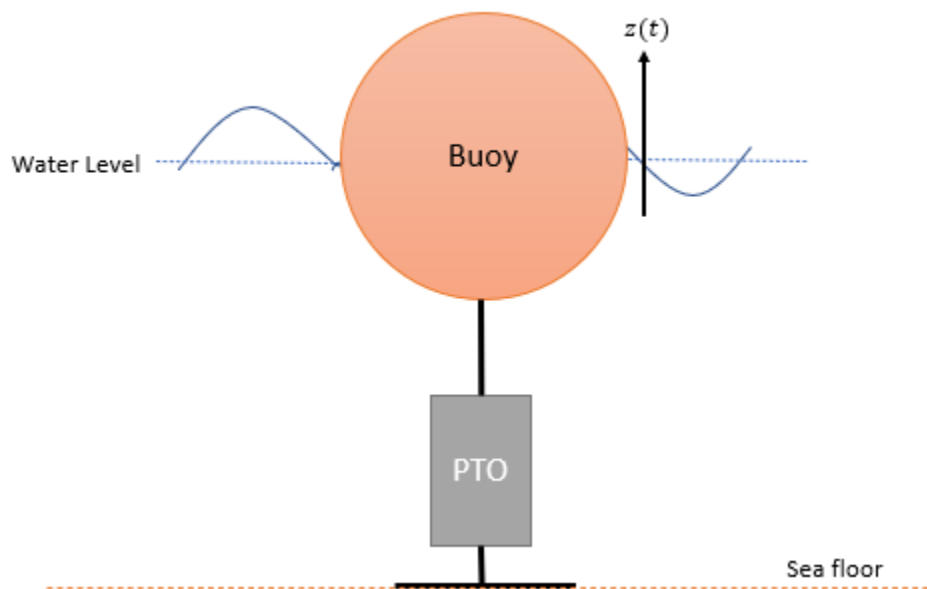


Figure 2.1. Spherical buoy point absorber WEC

A free body diagram of the buoy is shown in Figure 2.2 below where  $\mu$  is the added mass and represents a layer of water that surrounds and moves with the buoy [12]. The excitation force,  $F_{exc}$ , is caused by the incident waves. Depending on the model approach, it can also include effects such as diffraction and scattering. In this study, we are only

considering incident wave forces since the others are small in comparison [11]. The radiation damping is denoted as  $F_R$  and captures the transfer of kinetic energy from the buoy to the water. It should be noted that  $\mu$  and  $F_R$  are two terms from the total radiation force, but segregated based on their effect on buoy acceleration and speed. The hydrostatic force,  $F_h$ , is also known as the Archimedes force due to the displaced water volume.

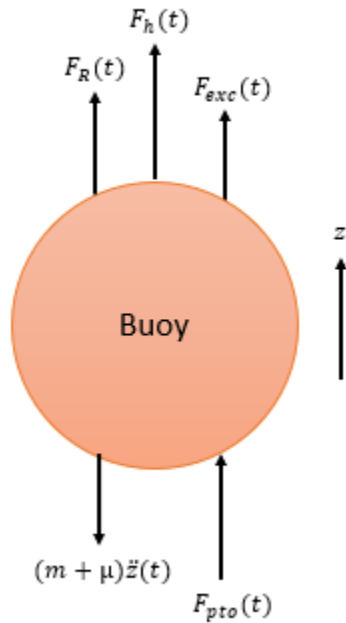


Figure 2.2. Sign conventions for forces acting on the spherical buoy of WEC

Applying Newton's Second Law to the free body diagram gives the WEC equation of motion can be –

$$(m + \mu)\ddot{z}(t) = F_{exc}(t) + F_h(t) + F_R + F_{pto}(t) \quad (1)$$

Many WEC control studies assume linear models for both  $F_{exc}$  and  $F_h$ . For example, if a spherical buoy, whose draught line is equal to its radius  $R$ , has small motion, then  $F_h$  can be approximated by a linear stiffness term,  $K_h \cdot z(t)$  where  $K_h = -\pi\rho gR^2$  where  $\rho$  is the density of water and  $g$  is the acceleration due to gravity. In this study both  $F_h$  and  $F_{exc}$  will be modeled using nonlinear expressions that account for the fact that the buoy's geometry is not cylindrical and thus both the hydrostatic and hydrodynamic forces are nonlinear in both the buoy's displacement,  $z(t)$  and the wave elevation,  $\eta$ . These forcing terms are called the nonlinear static and dynamic Froude-Krylov forces.

## Model Assumptions

1. The buoy only moves in the vertical direction
2. The PTO is ideal
3. The wave force is due to the incident waves
4. The incident wave profile is known in advance commensurate with the control horizon

The "truth model" used in this study will always use the nonlinear FK forces. Two versions of MPC will then be examined where the MPC's model uses: (1) linear FK forces, which is typically done in the literature, and (2) nonlinear FK forces. Before describing the MPC control system, more detailed development of  $F_h$  and  $F_{exc}$ , are provided below.

## 2.2 Static and Dynamic Nonlinear Froude-Krylov Forces

The nonlinear FK model used here is the same as described in [11]. Using a cylindrical coordinate parameterization of a buoy,

$$x = f(\sigma)\cos\theta$$

$$y = f(\sigma)\sin\theta$$

$$z = \sigma$$

where  $f(\sigma)$  is the sphere radius as a function of the vertical variable  $\sigma$ , they developed the general equation for the total (static and dynamic) FK force as

$$FFK = -2\pi\rho g \int_{(-R+z-\eta)}^{\eta} P \cdot f(\sigma) \cdot f'(\sigma) \cdot d\sigma$$

where  $\eta$  is wave elevation at the center of the buoy,  $P$  is the pressure exerted on the buoy by the water. The pressure was then approximated using

$$P = \rho g \eta e^{\chi\sigma} - \rho g z$$

where  $\chi$  is the wavenumber,  $\eta$  is the wave elevation. The first term in  $P$  generates the dynamic FK force and the second term produces the static FK force. For a sphere whose radius and draught lines are both  $R$  the expressions are:

$$fkS_{nl} = 2\pi\rho g \left[ \frac{\eta^3}{3} - z \cdot \frac{\eta^2}{2} - \frac{(z-h_o)^3}{3} + \frac{z(z-h_o)^2}{2} \right] - mg \quad (2)$$

$$fkD_{nl} = -2\pi \left\{ \eta\rho g \left[ \frac{e^{\chi\eta}(\chi\eta-1)}{\chi^2} + \frac{e^{-\chi(R-z)} \cdot (\chi(R-z)+1)}{\chi^2} \right] - \frac{\eta g \rho z (e^{\chi\eta} - e^{-\chi(R-z)})}{\chi} \right\} \quad (3)$$

As mentioned earlier, the truth model uses the nonlinear FK forces of Eq. 2 and Eq. 3. The MPC control comparison below considers the cases where the MPC model uses a linearized version of these equations, as compared to the nonlinear ones. The linear version of the static and dynamic FK forces are

$$fkS_{lin} = -\rho g \pi R^2 \cdot z(t) = -K_h \cdot z(t) \quad (4)$$

$$fkD_{lin} = 2\pi\rho g\eta \left[ \frac{1}{\chi^2} - \frac{e^{-R\chi}(R\chi+1)}{\chi^2} \right] \quad (5)$$

### Summary

The WEC truth model physical parameters are given in Table 1 where it's also indicated if they are independent or derived.

WEC parameters used –

Table 2.1 WEC parameters used to simulate spherical buoy

Sr No	Parameter	Notation	Value	Unit	
1	Radius	$R$	2.5	$m$	Independent
2	Draft	$h_o$	2.5	$m$	Independent
3	Mass	$m$	32725	$kg$	Derived from buoy geometry
4	Added Mass	$\mu$	14019	$kg$	Derived from WAMIT data
5	Radiation Damping Coefficient	$B$	9051.2	$N/(m/s)$	Derived from WAMIT data
6	Linear Hydrostatic Stiffness	$K_h$	192620	$N/m$	Derived from buoy geometry
7	Water Density	$\rho$	1000	$kg/m^3$	Independent



### 3 Model Predictive Controller

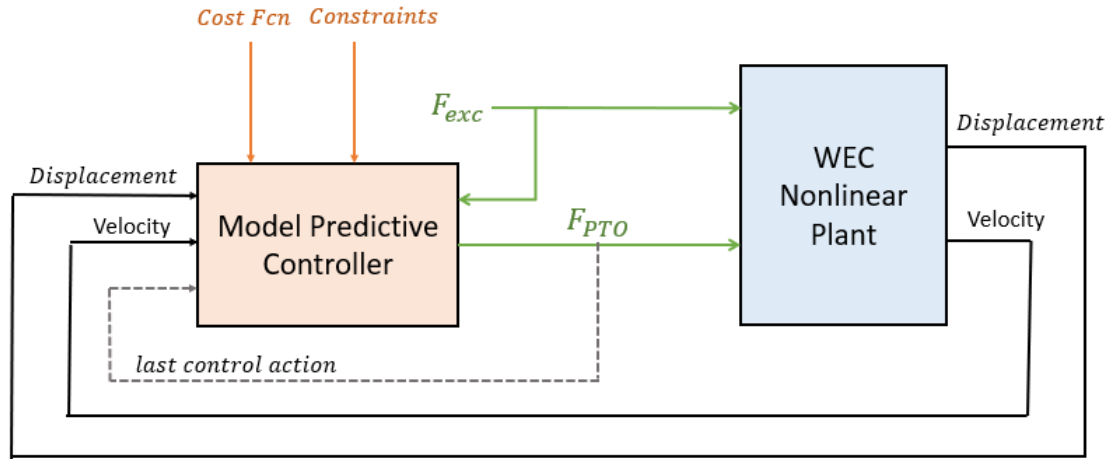


Figure 3.1. Block diagram of MPC for WEC

Model Predictive Control is an optimization problem with state constraints. Which is formulated as shown below –

The goal is to find optimal  $F_{pto}$  force vector that maximizes the absorbed energy

$$Energy = - \int_0^T F_{pto} \cdot \dot{z}(t) dT$$

Subject to dynamic WEC system of Eq 1. – and, depending on the MPC case considered, either Eq. 2 and Eq. 3 or Eq. 4 and Eq. 5 for the FK force models. Buoy displacement is constrained to

$$|z| < z_{max}$$

and the PTO force is constrained to

$$|F_{pto}| < F_{pto\ max}$$

At each time step, MPC needs an input of excitation force predicted in few seconds in the future, this time is called prediction horizon defined in the MPC problem. Based on available excitation force prediction, past control action, current states of WEC, and state constraints defined at each time step, MPC formulates its control action over the prediction horizon. Once control action is planned over the prediction horizon, the first control action is selected from the vector of PTO force planned over the prediction horizon and is implemented on WEC nonlinear model.

Table 3.1 MPC parameters used in simulation

Sr No	MPC Parameter	Value	Unit
1	Prediction Horizon	3	sec
2	Control Horizon	3	sec
3	Simulation Update Time	0.05	sec
4	Control Update Time	0.1	sec

In this report, the prediction horizon chosen is 3 sec, the control horizon is 3 sec, the simulation update time is 0.05 sec, and the control update time is 0.1 sec. The control action is updated after every 0.1 sec of simulation. Fpto constraint is  $\pm 150000$  N and Displacement constraint is  $\pm 1$  m. MPC can switch between LMPC and NLMPC. The control action is fed to a nonlinear WEC plant.

Table 3.2 Constraints used for MPC simulation

Sr No	MPC Parameter	Value	Unit
1	Displacement	$\pm 1$	m
2	PTO force	$\pm 150000$	N

## 4 Results And Discussions

Results of WEC motion, power, and energy absorbed by WEC with LMPC and NLMPC are discussed in this section.

### 4.1 Bang-Bang Control in MPC

In Optimal control problems, where control force is bounded between lower and upper bounds, it is possible that control force only switches between lower bound and upper bound. Which is a case of bang-bang control. This can be observed in MPC designed to simulate spherical-shaped buoy of WEC.

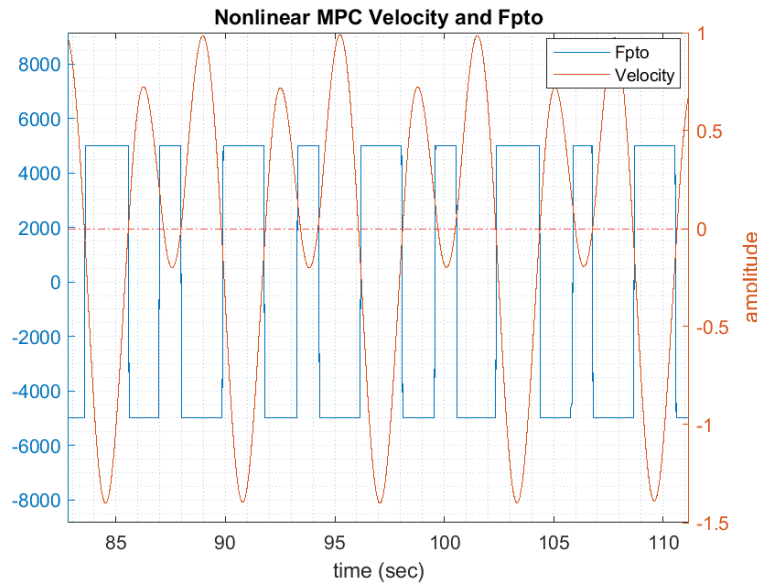


Figure 4.1.1. Bang-bang control of WEC with PTO force limit of  $\pm 5000$  N

Fig. 4.1.1. illustrates that MPC is extracting energy from WEC by keeping PTO force in phase with the velocity at each instant.

When PTO force is lowered at 5000 N, a classic bang-bang solution is obtained as shown in Fig. 4.1.1. However, due to less PTO force, the displacement of the WEC buoy does not reach its desired displacement limits. Hence, the PTO force limit is increased to  $\pm 150000$  N for the WEC buoy to hit the displacement limits of  $\pm 1$  m.

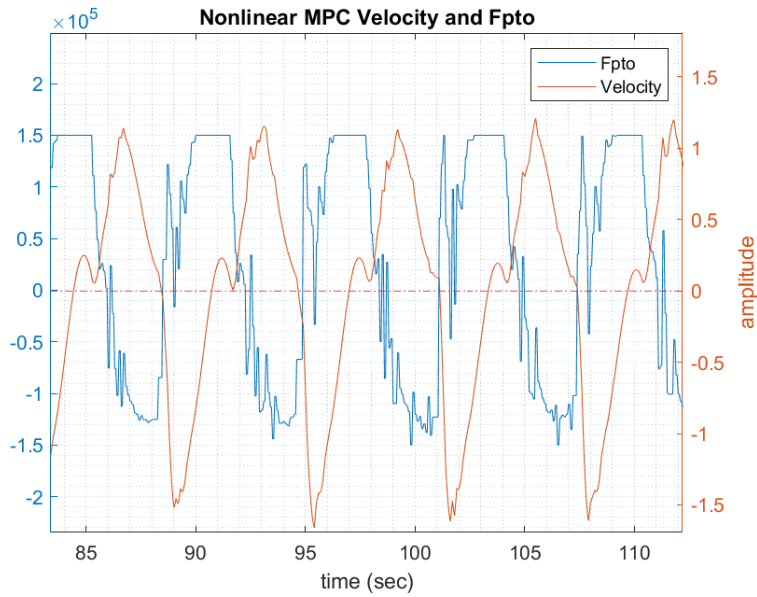


Figure 4.1.2. PTO force and velocity with PTO limits  $\pm 150000$  N.

With increasing PTO limits to push buoy to its displacement limit, it is observed that the MPC will not give an ideal bang-bang solution as shown in Fig. 4.1.2.

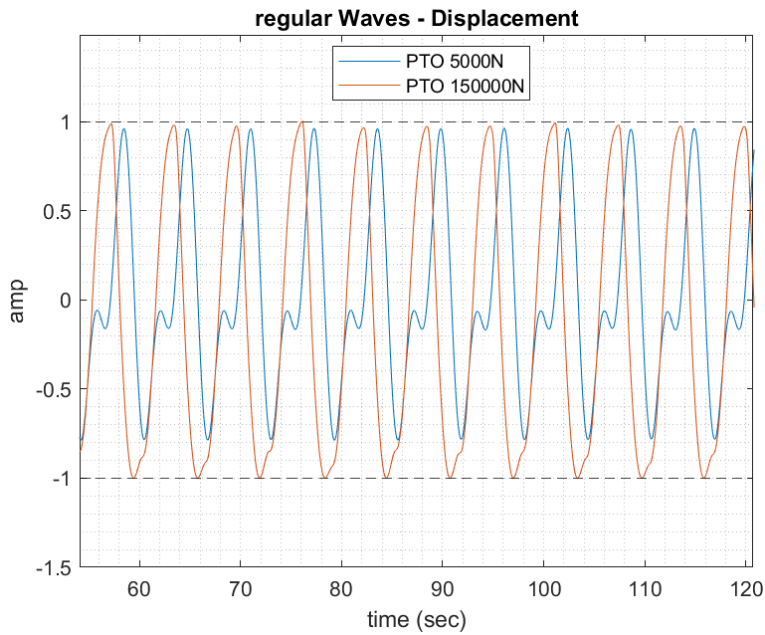


Figure 4.1.3. Comparison of displacement for PTO force limits of  $\pm 150000$ N Vs  $\pm 5000$ N

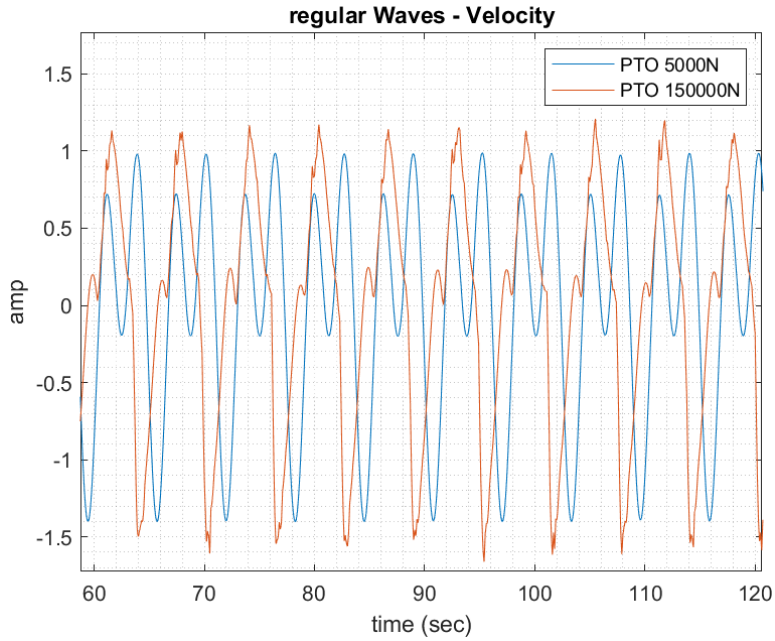


Figure 4.1.4. Comparison of velocity for PTO force limits of  $\pm 150000\text{N}$  Vs  $\pm 5000\text{N}$

From Fig. 4.1.3. and Fig.4.1.4., With increasing PTO limits to  $\pm 150000\text{ N}$ , displacement reaches the set limit of  $\pm 1\text{ m}$ . But at the same time, it is observed that large PTO force pushes the spherical buoy to its displacement limits and causes higher velocity amplitudes to harvest more energy from WEC.

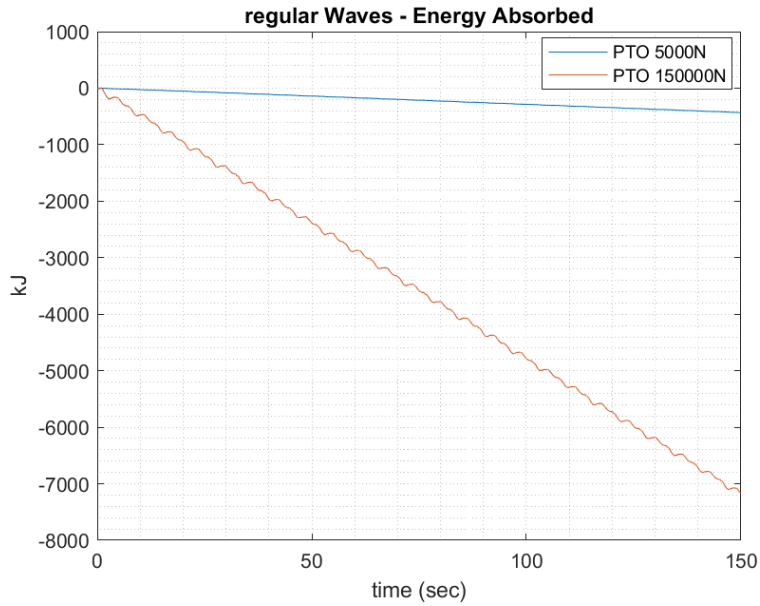


Figure 4.1.5. Comparison of energy absorbed with PTO force limits  $\pm 5000\text{N}$  and  $\pm 150000\text{N}$

As shown in Fig. 4.1.5., with increasing PTO limits, energy absorbed increases and yields nonideal bang-bang solution shown in Fig. 4.1.2.

## 4.2 MPC In Regular Waves

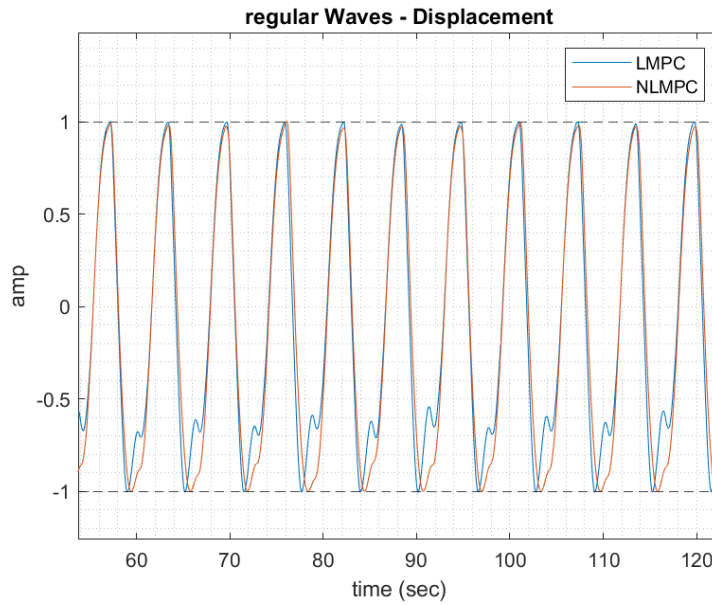


Figure 4.2.1. Comparison of displacement of WEC buoy for linear MPC vs NLMPC – regular waves

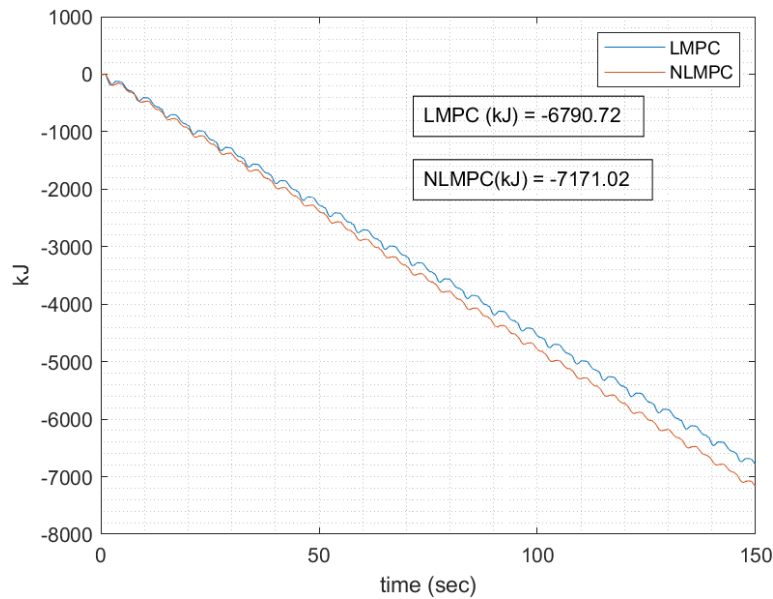


Figure 4.2.2. Energy absorbed in linear MPC and NLMPC for regular waves.

It is observed from Fig. 4.2.1. and Fig.4.2.2., as the LMPC model has not modeled the nonlinearity of the WEC plant correctly,

Energy harvested for regular waves in NLMPC is more than linear MPC by 5.6 % for the same PTO force and displacement limits.

### **4.3 Comparison of Nonlinear and Linear MPC Results**

Results of increasing PTO limits were discussed in section 4.1. A spherical buoy was simulated for regular waves and results using LMPC and NLMPC models controlling nonlinear WEC plant were compared in section 4.2.

From Fig 4.2.1., As the WEC plant dynamics is nonlinear, the LMPC and NLMPC both are able to keep the displacement within defined constraints at all points in the simulation.

From Fig. 4.2.1. – Fig. 4.2.2., it is observed that as both controllers are controlling the nonlinear WEC model with nonlinear hydrostatic stiffness coefficient, NLMPC performs better than LMPC model. NLMPC absorbs more energy when controlling the nonlinear WEC plant than linear MPC as shown in Fig. 4.2.2.

The velocity is not constrained in this simulation. Hence, increasing PTO limits will increase the velocity amplitudes to absorb more energy as shown in Fig. 4.1.4.

If the maximum excitation force of waves in a particular area of lakeshore or seashore is known, selecting a generator based on motion constraints and the maximum possible excitation force will help to extract maximum energy from the waves.

## 5 Conclusion

In this report, the NLMPC model uses realistic nonlinear Froude-Krylov hydrostatic and hydrodynamic forces whereas a LMPC uses linearized FK hydrostatic and linearized FK dynamic forces which has an assumption of smaller amplitudes of a buoy. These two models are compared against each other while controlling the same WEC plant which is subjected to nonlinear FK hydrostatic and FK hydrodynamic forces. Results of LMPC and a NLMPC are compared in section 4.2.

LMPC model is designed to work where the buoy is subjected to smaller amplitudes of motion. The nonlinearities become significant at larger amplitudes of excitation force which causes a higher amplitude of motion of buoy of the non-uniform cross-section..

It has been successfully demonstrated in this report that NLMPC controlling a nonlinear MPC plant will yield more energy than a LMPC model while keeping the state and PTO force constraints within defined limits. Modeling a controller replicating the correct nonlinear dynamics of a plant is beneficial when the plant experience dominant nonlinearities.

NLMPC is a clear choice for buoy's of non-uniform cross-sections subjected to higher displacements. LMPC can be implemented where waves are not aggressive and cause lower amplitudes of WEC buoy motion.

This simulation of MPC does not focus on real-time implementation on WEC. And the wave prediction is assumed ideal, future work will focus on implementing more realistic wave prediction algorithms which will benefit the practical implementation.



## 6 References

- [1] U.S. Energy Information Administration (EIA), "International Energy Outlook", Internet : <<https://www.eia.gov/outlooks/ieo/pdf/ieo2020.pdf>>, Oct 2020.
- [2] I. López, J. Andreu, S. Ceballos, I. Martínez de Alegría, I. Kortabarria, "Review of wave energy technologies and the necessary power-equipment", *Renewable and Sustainable Energy Reviews*, 27, pp 413–434, 2013.  
<<https://doi.org/10.1016/j.rser.2013.07.009>>
- [3] A. Clément, P. McCullen, A. Falcão, A. Fiorentino, F. Gardner, F., K. Hammarlund, G. Lemonis, T. Lewis, K. Nielson, S. Petroncini, M. T. Pontes, P. Schild, B-O. Sjöström, H. C. Sørensen and T. Thorpe, "Wave energy in Europe: current status and perspectives". *Renewable and sustainable energy reviews*, 6, pp 405-431, 2002.
- [4] R. Henderson, "Design, simulation, and testing of a novel hydraulic power take-off system for the Pelamis wave energy converter", *Renewable Energy*, vol. 31, issue. 2, pp 271-283, 2006 <<https://doi.org/10.1016/j.renene.2005.08.021>>
- [5] J. Hals, J. Falnes, and T. Moan, "Constrained Optimal Control of a Heaving Buoy Wave-Energy Converter." *Journal of offshore Mechanics and Arctic Engineering, ASME*, 2011. < <https://doi.org/10.1115/1.4001431>>
- [6] T. K. A. Brekken, "On model predictive control for a point absorber wave energy converter.", *IEEE Trondheim PowerTech. IEEE*, 2011.  
<<https://ieeexplore.ieee.org/abstract/document/6019367>>
- [7] F. Fusco and J. V. Ringwood. "Short-term wave forecasting for real-time control of wave energy converters.", *IEEE Transactions on sustainable energy 1.2*, pp. 99-106, 2010. <<https://ieeexplore.ieee.org/abstract/document/5451110>>
- [8] F. Fusco and J. V. Ringwood, "A study of the prediction requirements in real-time control of wave energy converters.", *IEEE Transactions on Sustainable Energy 3.1*, pp 176-184, 2011 <<https://ieeexplore.ieee.org/abstract/document/6102286>>
- [9] E. Anderlini, D.I.M. Forehand, E. Bannon, and M. Abusara, "Reactive control of a wave energy converter using artificial neural networks", *International Journal of Marine Energy*, vol. 19, pp- 207-220, 2017 <<https://doi.org/10.1016/j.ijome.2017.08.001>>
- [10] J. A. M. Cretel, G. Lightbody, G. P. Thomas and A. W. Lewis, "Maximisation of energy capture by a wave-energy point absorber using model predictive control.", *IFAC Proceedings*, vol. 44.1, pp 3714-3721., 2011.  
<<https://www.sciencedirect.com/science/article/pii/S1474667016441893>>
- [11] G. Giuseppe, and J. V. Ringwood., "Computationally efficient nonlinear Froude–Krylov force calculations for heaving axisymmetric wave energy point

absorbers", *Journal of Ocean Engineering and Marine Energy* 3.1, pp 21-33., 2017. <  
<https://link.springer.com/article/10.1007/s40722-016-0066-2> >

[12] U. A. Korde, and J. V. Ringwood, "Hydrodynamic Control of Wave Energy Devices", Cambridge University Press, 2016.

[13] J. Falnes, "*Ocean Waves and Oscillating Systems*", Cambridge University Press., 2002.

[14] E. Weisstein, "Spherical Cap", *MathWorld- A Wolfram Web*, Internet :  
<<https://mathworld.wolfram.com/SphericalCap.html>> [March18, 2021].